Journal of Histochemistry & Cytochemistry 61(2) 169–176

DOI: 10.1369/0022155412468590
http://jhc.sagepub.com
SAGE

Relation between Ultrastructural Localization, Changes in Caveolin-1, and Capillarization of Liver Sinusoidal Endothelial Cells in Human Hepatitis C–Related Cirrhotic Liver

Hitoshi Yamazaki, Masaya Oda, Yoshihito Takahashi, Hiroyoshi Iguchi, Kazunori Yoshimura, Nobuhiko Okada, and Hiroaki Yokomori

Departments of Pathology (HYamazaki), Surgery (YT), Radiology (HI), and Internal Medicine (HYokomori), Kitasato University Medical Center, Kitasato University, Saitama, Japan; Organized Center of Clinical Medicine, International University of Health and Welfare, Tokyo, Japan (MO); Department of Rehabilitation, Nihon Institute of Medical Science, Saitama, Japan (KY); and Department of Microbiology, School of Pharmacy, Kitasato University, Tokyo, Japan (NO)

Summary

Most vascular endothelial cells are continuously exposed to shear stress in vivo. Caveolae are omega-shaped membrane invaginations in endothelial cells (ECs) and are enriched in cholesterol, caveolins, and signaling molecules. This study was designed to elucidate the ultrastructural localization and change in caveolin-1 expression within human liver sinusoidal endothelial cells (LSECs) during the progression of cirrhosis caused by hepatitis C, using tissue sections prepared via perfusion-fixation. Normal control liver specimens and hepatitis C–related Child-Pugh A and C cirrhotic liver specimens were studied. Caveolin-1 in the liver sinusoids was examined via immunohistochemistry, Western blotting, and immunoelectron microscopy. In control liver tissue, caveolin-1 was localized on caveolae mainly in arterial and portal endothelial cells of the portal tract and was also found on vesicles and some fenestrae in LSECs around the central vein. In cirrhotic liver tissue, aberrant caveolin-1 expression was observed on caveolae-like structures in LSECs. Caveolin-1 was especially overexpressed in late-stage cirrhosis. This study demonstrates that caveolin-1 is strongly expressed within caveolae-like structures and associated vesicles within LSECs of the hepatitis C–related cirrhotic liver. These findings suggest a direct association of caveolin-1 in the process of differentiation of LSECs in cirrhosis-mediated capillarization. (J Histochem Cytochem 61:169–176, 2013)

Keywords

caveolin-1, human liver cirrhosis, perfusion fixation method, immunoelectron microscopy

Biomechanical forces such as shear stress, cyclic strain, and hydrostatic pressure are highly relevant to normal and pathological endothelial cell function (Davies 1995). Caveolae are 50- to 100-nm, omega-shaped membrane invaginations on endothelial cells (ECs) and are plasmalemmal domains enriched in cholesterol, caveolins, and signaling molecules (Parton and Simons 2007). When ECs are subjected to shear stress, the density of caveolae in the cell membrane increases, modulating the activation of signaling pathways (Boyd et al. 2003). Many of these functions are reliant to a lesser or greater extent on the caveolae marker protein and on the key structural and functional protein caveolin-1. The identification of caveolin-1 (a 22-kD integral membrane protein) as the major component of caveolar membranes (Rothberg et al. 1992) has allowed these caveolar vesicles to be identified immunocytochemically in a variety of cells such as fibroblasts and endothelial cells (Rothberg et al. 1992; Rajamannan et al. 2002). However, most vascular endothelial cells in vivo are continuously exposed to shear stress, and statically cultured cells may not represent true "in vivo normal

Received for publication July 27, 2012; accepted October 19, 2012.

Corresponding Author:
Hiroaki Yokomori, MD, Department of Internal Medicine, Kitasato Medical Center Hospital, Kitasato University, Saitama, 364-8501, Japan.
E-mail: yokomori@insti.kitasato-u.ac.jp

conditions." Although statically cultured cells have been extremely valuable in elucidating endothelial responses to mechanical force, their phenotypes and responses may not mimic the exact physiological conditions occurring in vivo (Schnitzer et al. 1994). The number of caveolae in endothelial cells decrease during culture compared with their counterparts in vivo (Schnitzer et al. 1994).

Angiogenesis is the process by which new vasculature is derived from preexisting blood vessels. Previous studies have proposed a role for caveolin-1 in the regulation of angiogenesis and sinusoidal differentiation (Griffoni et al. 2000; Liu et al. 2002; Yokomori et al. 2009). Ultrastructurally, perfusion-fixation rather than immersion-fixation of empty vessels and sinusoids is essential in preserving the fine structure and architecture of the liver. Perfusion fixation has been the gold standard, especially in the study of the sinusoids and sinusoidal cells in experimental animals and humans (Wisse 1972). In addition, perfusion-fixation has several advantages such as fixing structures of organelles and molecules in their in vivo positions and ensuring stability during further processing (Wisse et al. 2010).

In this study, we detailed the in vivo localizations of caveolin-1 in normal versus cirrhotic human liver by immunoelectron microscopy specimens using perfusion-fixation and tangential sections of liver sinusoidal endothelial cells (LSECs).

Materials and Methods

Materials

With the aim to elucidate the localization and changes in caveolin-1 expression during the progression of cirrhosis, we studied three groups of specimens: normal liver tissue, as well as liver tissues from early stage and advanced stage cirrhosis caused by hepatitis C. As controls, wedge biopsy specimens were obtained from the normal portions of the livers from four patients (four male; aged 64–70 years, mean 67 years) who underwent surgical resection for metastatic liver carcinoma (three colonic carcinomas, one cholangiocarcinoma, and one sclerosed hemangioma). Cirrhotic liver specimens were obtained from gross cirrhotic portions surgically resected from five patients (two males and three females; aged 61–74 years, mean 67.4 years) who underwent hepatectomy for hepatocellular carcinoma (HCC) with concurrent hepatitis C–related cirrhosis. Each patient was evaluated before the operation with an indocyanine green (ICG) clearance test and Child-Pugh grading (Lam et al 1999). All patients had ICG clearance <15% and were classified as Child-Pugh grade A. This group was designated Child-Pugh A group. All resected HCCs were capsulated and clearly demarcated from the cirrhotic part of the liver. Cirrhotic samples were obtained from sites as far away from the HCC as possible.

Furthermore, liver tissues were obtained from five autopsy cases (four males and one female; aged 61–79 years, mean 75.8 years), in which autopsies were performed within 3 hr after death. All cases were diagnosed as HCC with concurrent hepatitis C–related cirrhosis and classified as Child-Pugh grade C. This group was designated Child-Pugh C group. Informed consent for the use of surgically resected tissues was obtained from each patient in the normal and Child-Pugh A groups. Informed consent for autopsy was obtained from the families of the deceased patients in the Child-Pugh C groups. This study was approved by the Ethics Committee of the Kitasato Institute Medical Center Hospital, Kitasato University (No. 23-22).

Fibrosis Grades of Cirrhotic Specimens

To relate the morphological cirrhotic changes with Child-Pugh scores, we performed hematoxylin and eosin and Mallory-Azan staining on sections prepared from Child-Pugh A and Child-Pugh C cirrhotic liver specimens. In Child-Pugh A specimens, the fibrous septa surrounding regenerative nodules were rather thin and sometimes incomplete, corresponding to hepatic fibrosis grades 2 to 3. In Child-Pugh C specimens, the fibrous septa were thicker with more extensive pericellular fibrosis, larger regenerative nodules, and more abundant microvascular proliferation, corresponding to hepatic fibrosis grade 3 and above.

Immunohistochemistry

Liver tissue samples with a size of approximately 4 × 3 × 1.5 cm were fixed in formalin and embedded in paraffin. Then, 4-μm sections were cut from the paraffin blocks, deparaffinized with xylene, and hydrated using graded ethanol. They were incubated overnight at 4C with 1:200 dilution of rabbit anti–caveolin-1 polyclonal antibody (sc-894; Santa Cruz Biotechnology, Santa Cruz, CA). Then the sections were incubated with EnVision reagents (Dako, Inc., Tokyo, Japan) at room temperature for 30 min. After repeated washing with phosphate-buffered saline (PBS), the sections were reacted with diaminobenzidine containing 0.01% H_2O_2 and counterstained with hematoxylin for light microscopic study.

Western Blotting

The tissue sample was homogenized in 10 volumes of homogenization buffer (20 μM Tris-HCl [pH 7.5], 5 mM $MgCl_2$, 0.1 mM PMSF, 20 μM pepstatin A, and 20 μM leupeptin) using a polytron homogenizer at setting 7 for 90 sec. The membrane proteins obtained were used for immunoblotting. Proteins (30 μg/ml) were separated on SDS/PAGE and transferred onto polyvinylidene difluoride membranes (NTN Life Science Products Inc., Frederick, Colorado, USA). The blots were blocked with 5% (w/v) dried milk in PBS for 30 min and incubated with anti–caveolin-1 antibody diluted 1:5000 in 0.1% Tween-20 in PBS. The

blots were washed and incubated for 1 hr at room temperature with a horseradish peroxidase–conjugated goat anti-rabbit IgG (Santa Cruz Biotechnology). Protein bands were detected using an enhanced chemiluminescence detection system (ECL Plus; Amersham Biosciences, Uppsala, Sweden) after exposing the nitrocellulose sheets to Kodak XAR film (Kodak; Rochester, NY). Alpha-tubulin was used as a loading control for Western blot analysis.

Immunogold-Silver Staining Method for Electron Microscopy

We used a modified perfusion-fixation method to fix the structures of organelles and molecules in their in vivo positions (Wisse et al. 2010). In brief, wedge biopsies of roughly 3 × 1 × 1 cm were obtained from the margin of a liver lobe as soon as the operator had access to the control or Child-Pugh A cirrhotic liver. The tissue was immediately transferred to a container and filled with PBS (pH 7.4) at 37C. Perfusion-mediated injection of periodate-lysine-paraformaldehyde (PLP) fixative was performed in a Petri dish filled with saline. The wedge biopsy was held at a corner by forceps, and PLP was injected by a 26-gauge syringe from multiple sides until discoloration and hardening of the tissue were obtained. After perfusion and incubation with PLP overnight at 4C, semi-thin 1-mm sections were prepared and (1) immersed for 15 min in three changes of 0.01% PBS (pH 7.4), (2) incubated with anti–caveolin-1 antibody diluted 1:200 in 0.01M PBS containing 1% bovine serum albumin overnight at 4C in a moisture chamber, (3) treated for 15 min in PBS three times, (4) incubated in 1.4 nm colloidal gold–conjugated anti-rabbit IgG antibody (Nanogold; Nanoprobes, Inc., Yaphank, NY) diluted 1:40 for 40 min, and (5) physically developed using a silver enhancement kit (Nanoprobe Silver Enhancement Kit; Nanoprobes, Inc.) (Humbel et al. 1995; Yokomori et al. 2011). The liver sections were washed with three changes of 0.01% PBS and fixed in 1.5% glutaraldehyde buffered with 0.01% phosphate buffer (pH 7.4) for 1 hr at 4C, followed by a graded series of ethanol solutions and postfixation with 2% osmium tetroxide in 0.01% phosphate buffer (pH 7.4). After embedding in Epon, ultrathin sections were cut using a diamond knife on an LKB ultra microtome. They were stained with uranyl acetate and observed under a transmission electron microscope (JEM-1200 EX; JEOL, Tokyo, Japan) with 80-kV acceleration voltage.

Results

Immunohistochemical Distribution of Caveolin-1

In control liver tissue, immunohistochemistry revealed caveolin-1 in the hepatic artery, capillary venules, and portal vein in the portal tract. Caveolin-1 was also detected in the hepatic sinusoidal lining cells around pericentral zone 3 in control liver tissue (Fig. 1a–c).

In Child-Pugh A cirrhotic liver (early stage), immunostaining of caveolin-1 was evident mainly at sites of proliferated capillary arteries and sinusoidal lining cells in the peripheral regions of nodules (Fig. 1d–f). In Child-Pugh C cirrhotic liver (late stage), the intensity of caveolin-1 immunoreactivity was enhanced mainly on sinusoidal lining cells in regenerated nodules and in the peripheral regions of nodules and fibrous septa. Caveolin-1 immunoreactivity was more intense in severely fibrotic tissues (Fig. 1g–i).

Western Blotting

To confirm the immunohistochemical results, we investigated the caveolin-1 protein expression in normal and cirrhotic liver tissues using Western blotting. Caveolin-1 protein was expressed abundantly in Child-Pugh A and C cirrhotic liver and scantily in control liver tissues (Fig. 2).

Immunoelectron Microscopic Findings

In control liver, underneath the thin layer of fenestrated endothelium, the space of Disse showed the presence of microvilli. The fenestrae in such preparations had an average diameter of approximately 125 nm. Immunogold particles showing caveolin-1 immunoreactivity indicated the presence of many caveolae in capillary and vascular endothelial cells (Figs. 3 and 4) and scanty caveolae in liver sinusoidal endothelial cells around the portal tract (Fig. 5). Immunogold particles indicating caveolin-1 were found in vesicles or vacuoles and a few fenestrae around the central vein (Fig. 6).

In cirrhotic liver, immunogold particles indicating caveolin-1 were observed in caveolae-like structures and vesicles (Figs. 7 and 8) and sparsely identified in vacuoles (Fig. 8) in capillarized liver sinusoidal endothelial cells.

Discussion

In this study, we investigated the ultrastructural localization of caveolin-1 on vascular capillary ECs and LSECs using perfusion-fixation and immunoelectron microscopy, which may provide insight into the role of caveolin-1 in the cirrhosis process.

In terms of permeability, Nanogold particles can penetrate 15-μm-thick sections throughout their thickness (Sawada and Ezaki 1993). It is also known that smaller probes yield more intense labeling (Baschong et al. 1998). Therefore, the use of Nanogold is more beneficial than other larger probes. A study reported that the Nanogold technique (Sawada and Ezaki 2000) yielded more intense labeling when compared with the ultrathin cryosection technique using the same primary antibody and 10 nm colloidal gold (Yazama et al. 1997), although a direct comparison was not possible due to methodological differences.

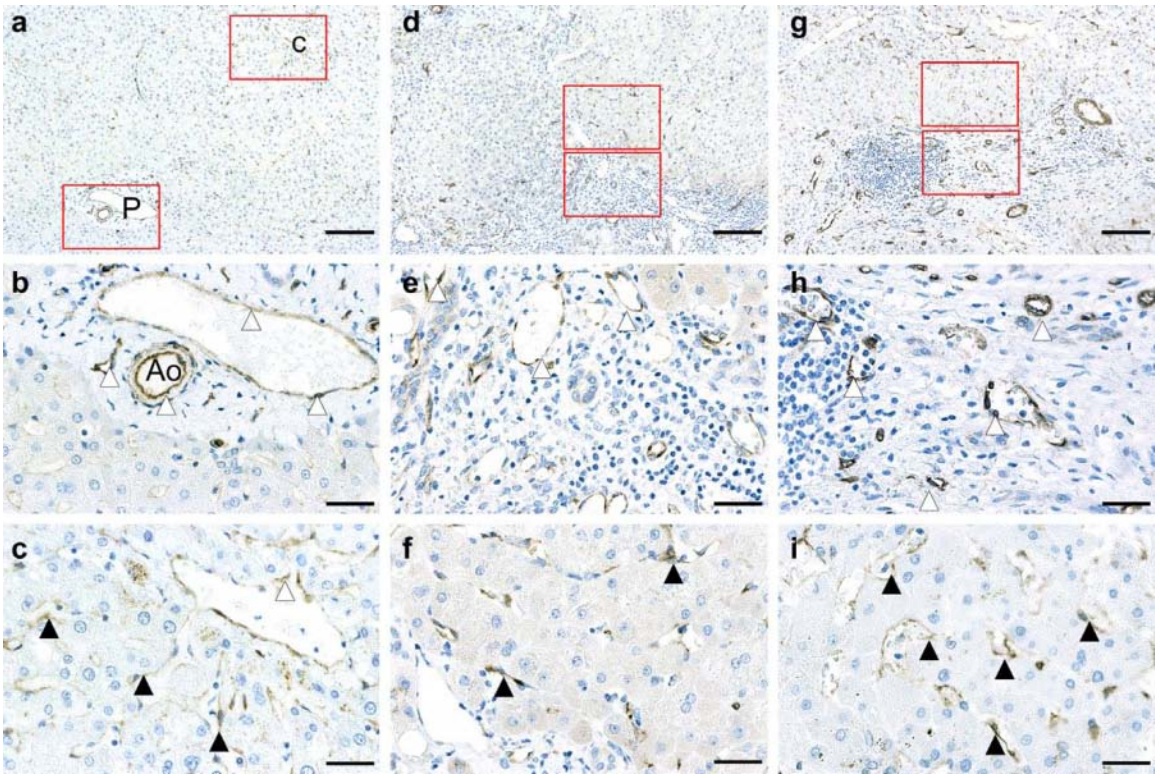

Figure 1. Immunohistochemical distribution of caveolin-1 in control liver (a–c), Child-Pugh A cirrhotic liver (d–f), and Child-Pugh C cirrhotic liver (g–i). P, portal tract; C, central vein; Ao, hepatic artery. White arrowheads denote hepatic artery or central vein or portal vein. Black arrowheads denote hepatic sinusoid. (a–c) Control liver tissue. Immunohistochemistry revealed caveolin-1 in the hepatic artery, capillary venule, and portal vein in the portal tract (P) and is detected in the hepatic sinusoidal lining cells around pericentral zone 3. (a) Low magnification. (b) High magnification of periportal region. (c) High magnification of pericentral region. (d–f): Child-Pugh A liver tissue. In early stage cirrhotic liver, caveolin-1 expression is evident mainly at sites of proliferated capillary arteries and sinusoidal lining cells in the peripheral regions of nodules. (d) Low magnification. (e) High magnification of regenerated fibrotic region. (f) High magnification of hepatic sinusoid. (g–i) Child-Pugh C liver tissue. In late-stage cirrhotic liver, the intensity of caveolin-1 immunoreactivity is enhanced mainly on sinusoidal lining cells in the regenerated nodules and in peripheral regions of nodules and fibrous septa. Caveolin-1 immunoreactivity is more intense in severely fibrotic tissue. (g) Low magnification. (h) High magnification of regenerated fibrotic region. (i) High magnification of hepatic sinusoid. Bar = 153 μm for a, d, and g. Bar = 32 μm for b, c, e, f, h, and i.

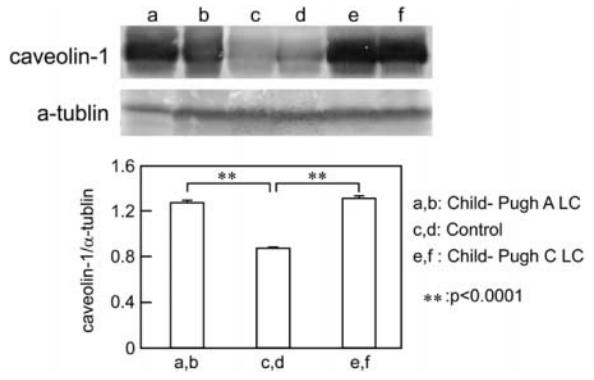

Figure 2. Western blot analysis of caveolin-1 protein in human control and cirrhotic liver tissues. Samples containing 30 μg protein were subjected to SDS-PAGE and analyzed by Western blotting. Lanes a and b show Child-Pugh A cirrhotic liver samples. Lanes c and d show control liver samples. Lanes e and f show Child-Pugh C cirrhotic liver samples. Caveolin-1 protein expression is significantly more intense in Child-Pugh A and C cirrhotic liver compared with control.

Expression of caveolin-1 around zone 3 in normal human liver has been reported (Yokomori et al. 2002). Recently, Warren et al. (2010) demonstrated in caveolin-1 knockout and wild-type mice that the structure of fenestrations in the liver sinusoidal endothelium does not depend on caveolin-1 and that fenestration is not a form of caveola. The report of Biazik et al. (2011) on tubular structures located within the cytoplasm of lizard liver sinusoidal endothelium generated new ultrastructural insights related to the caveolae and associated cytoplasmic tubular structures in LSECs.

The localization of caveolin-1 might include almost all cellular organelles in LSECs involved in endocytosis and intracellular trafficking (Smedsrød et al. 1985). Moreover, caveolin-1 expression was detected around zones 2 to 3 in normal liver (Yokomori et al. 2002). By immunoelectron microscopy using the postembedding method, electron-dense particles showing the presence of caveolin-1 were located on the plasma membrane of fenestrae in LSECs isolated from normal rats (Ogi et al. 2003), although the

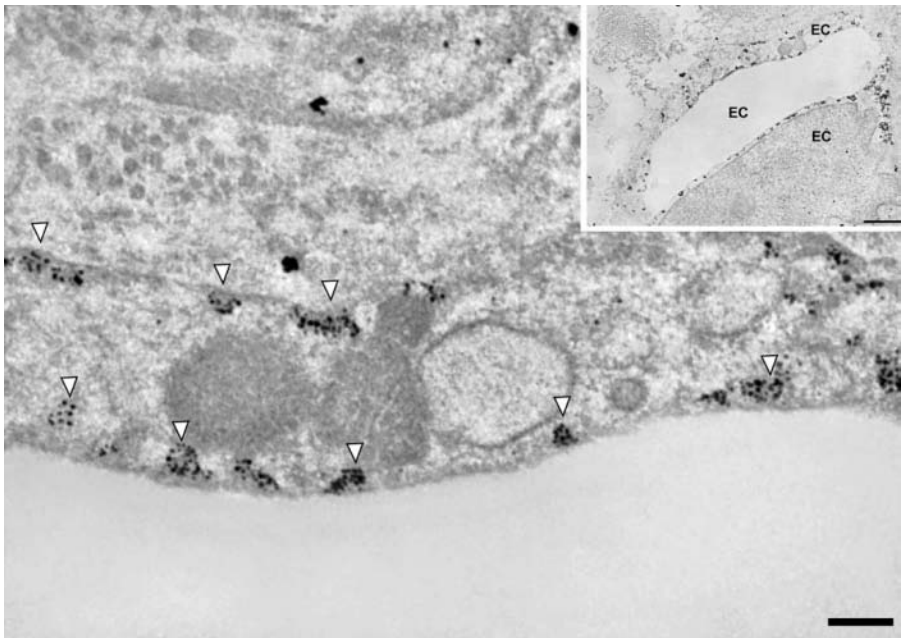

Figure 3. Transmission electron micrographs showing capillary endothelial cells in normal control liver tissue. Immunogold particles indicating caveolin-1 are observed in caveolae and partly some vesicles in capillary endothelial cell. Inset shows lower magnification. EC, capillary endothelial cell. Magnification: ×20,000 (bar: 200 nm). Inset magnification: ×2000 (bar: 1 µm). White arrowheads denote caveolae.

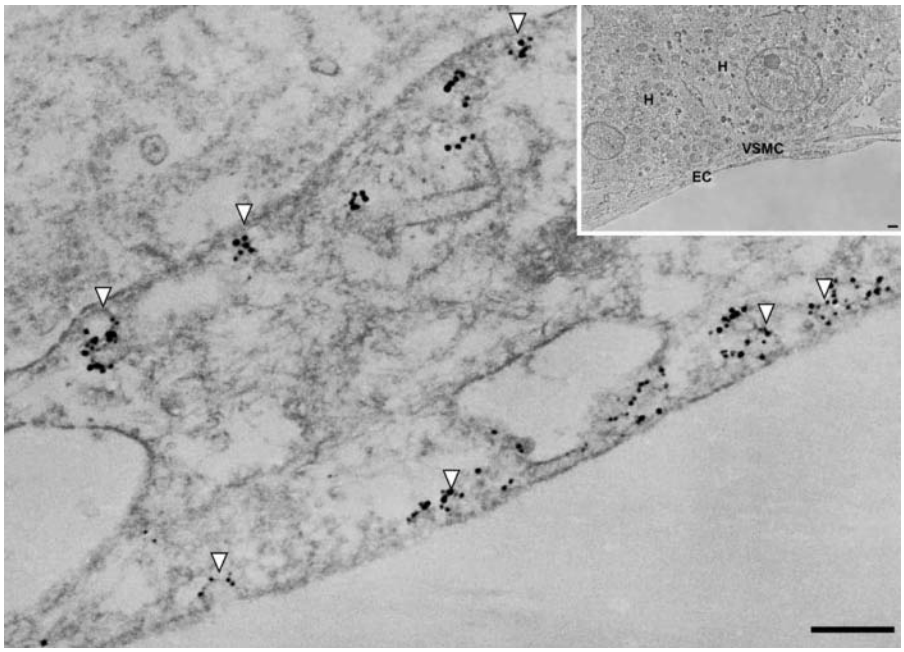

Figure 4. Transmission electron micrographs showing portal venue in normal control liver tissue. Immunogold particles indicating caveolin-1 are found in caveolae in endothelial cells of the portal venule. EC, endothelial cell of the portal venule; H, hepatocyte; VSMC, vascular smooth muscle cell. Magnification: ×20,000 (bar: 200 nm). Inset shows lower magnification: ×2000 (bar: 1 µm). White arrowheads denote caveolae.

statically cultured LSECs may not represent the true in vivo normal condition. The results obtained from the present study suggest that in human control liver, caveolin-1 is localized on vesicles derived from Golgi complexes and sparsely on sinusoidal endothelial fenestrae in the nearby central vein. LSECs have a high endocytic capacity. This function of LSECs is reflected morphologically by the presence of numerous micro-pinocytotic vesicles and many lysosome-like vacuoles (Wisse 1972). Moreover, demonstration of clathrin-coated vesicles (Ogi et al. 2003) and stabilin-1/2–positive early endosomes (Schledzewski et al. 2011) along a microtubule network in LSECs links LSEC morphology to endocytic function. As described by Smedsrød et al. (1985), several factors make LSECs such effective and important scavengers. The liver, and therefore the LSEC, is the first checkpoint for macromolecules and antigens that enter the portal circulation from the intestine. LSEC clearance is facilitated by the slow and intermittent flow through the sinusoids, the large surface area of LSECs, the numerous positively charged coated pits that aid endocytosis of negatively charged molecules, and the presence of three distinct endocytosis receptors. Aging-related pseudocapillarization and liver disease–related capillarization both lead to a decline in endocytosis (Ito et al. 2007).

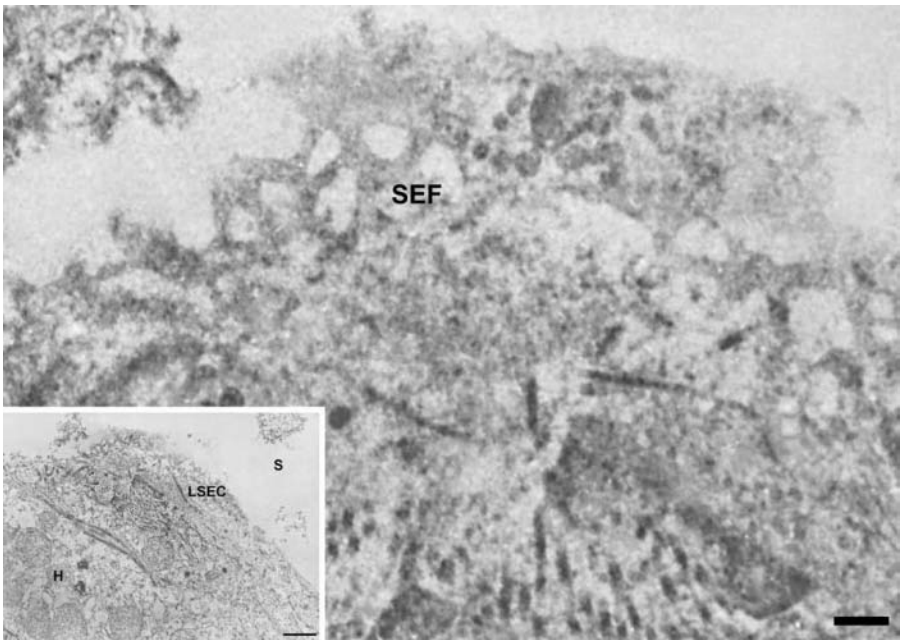

Figure 5. Transmission electron micrographs showing liver sinusoidal endothelial cells around the portal tract in normal control liver tissue. Underneath the thin layer of fenestrated endothelium, the space of Disse shows the presence of microvilli and thin fibers of reticulin. Sinusoidal endothelial fenestrae have an average diameter of about 125 nm. Immunogold particles indicating caveolin-1 are found sparsely in liver sinusoidal endothelial cells. LSEC, liver sinusoidal endothelial cell; SEF, sinusoidal endothelial fenestrae; H, hepatocyte; S, hepatic sinusoid. Magnification: ×20,000 (bar: 200 nm). Inset shows lower magnification: ×2000 (bar: 1 μm).

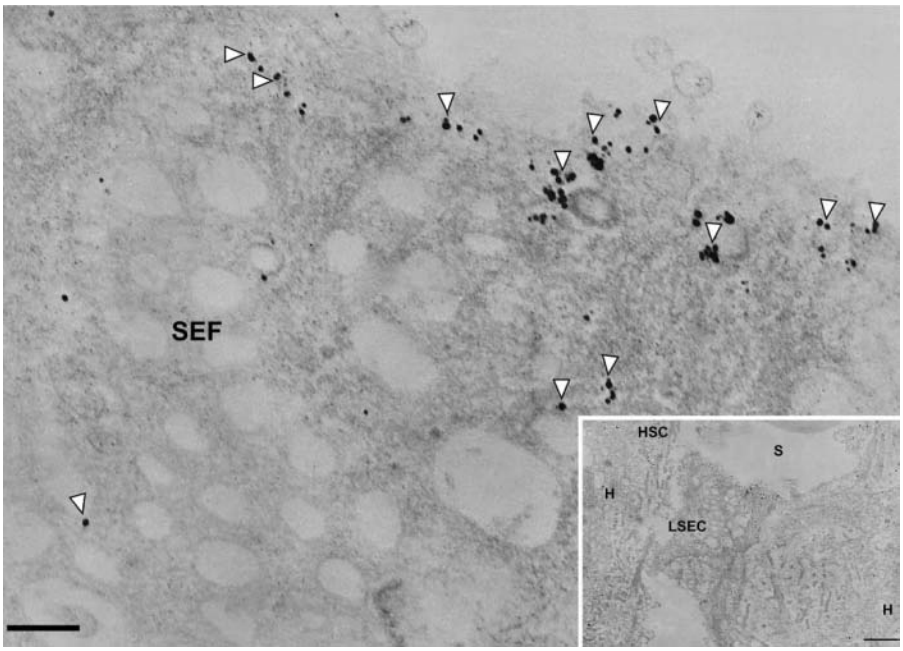

Figure 6. Transmission electron micrographs showing liver sinusoidal endothelial cells around the central vein in normal control liver tissue. Immunogold particles indicating caveolin-1 are found in vesicles and sparsely in fenestrae of liver sinusoidal endothelial cells. LSEC, liver sinusoidal endothelial cell; HSC, hepatic stellate cell; SEF, sinusoidal endothelial fenestrae; H, hepatocyte. Magnification: ×20,000 (bar: 200 nm). Inset shows lower magnification: ×2000 (bar: 1 μm). White arrowheads denote vesicles.

In an experiment aiming to detect caveolin expression in LSECs in intact tissue, bile duct ligated or sham rat liver sections were prepared for immunogold examination using transmission electron microscopy. Caveoin-1 was localized mainly on non–clathrin-coated endothelial cell vesicles in sham rat liver sinusoidal endothelial cells. On the other hand, caveolin-1 was expressed more prominently in bile duct-ligated liver and was localized on plasma membranes (Hendrickson et al. 2003).

In liver disease, LSECs exhibit swelling of the cytoplasm; protrusion of the cell body into the sinusoidal lumen; an increase in micro-pinocytotic vesicles; an appearance of numerous dense bodies and subsequent changes, including enlargement of the Golgi complex; an increase in rough endoplasmic reticulum in cytoplasmic processes closely related to basement membrane–like material; and reticulin fibers in the space of Disse (Bardadin and Desmet 1985; Iwamura et al. 1994). In our study, caveolin-1 expression was observed on caveola-like structures and a few vesicles in LSECs of patients with cirrhosis. LSECs in cirrhotic liver tissues are different from normal LSECs; their vacuolar apparatus (pinocytotic vesicles, endosomes, lysosomes, Golgi apparatus) is not developed. Furthermore, LSECs are lined by a thin, continuous basal lamina that is not present in

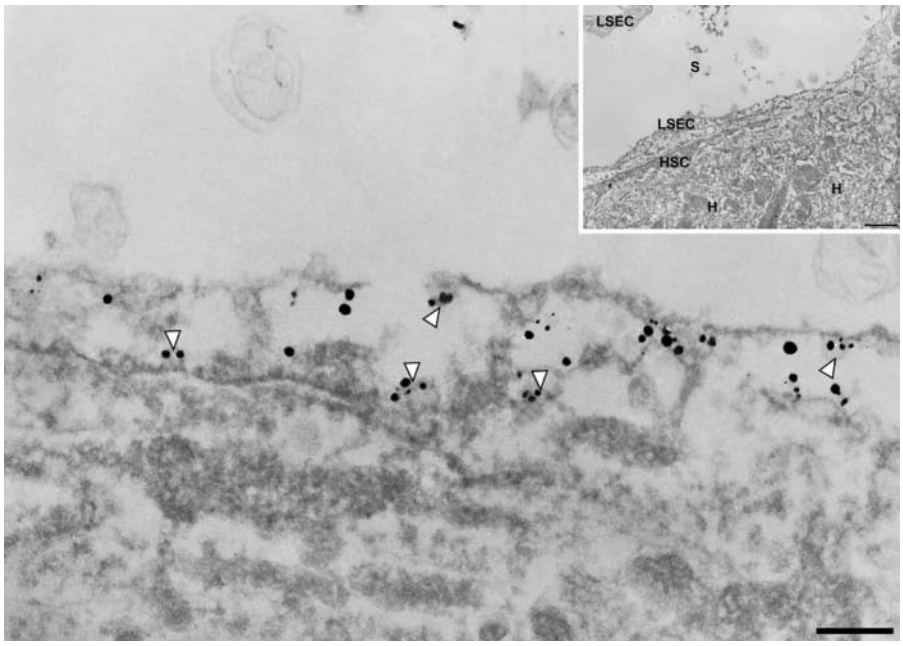

Figure 7. Transmission electron micrographs showing capillary, vascular, and liver sinusoidal endothelial cells in cirrhotic liver tissue. In cirrhotic liver, capillarized sinusoidal endothelial cells are different from normal sinusoidal endothelial cells; their vacuolar apparatus (pinocytotic vesicles, endosomes, lysosomes, Golgi apparatus) is not developed. Immunogold particles indicating caveolin-1 are found in caveola-like structures in capillarized liver sinusoidal endothelial cells. LSEC, liver sinusoidal endothelial cell; HSC, hepatic stellate cell; H, hepatocyte; S, hepatic sinusoid. Magnification: ×20,000 (bar: 200 nm). Inset shows lower magnification: ×2000 (bar: 1 μm). White arrowhead denotes caveolae-like structure.

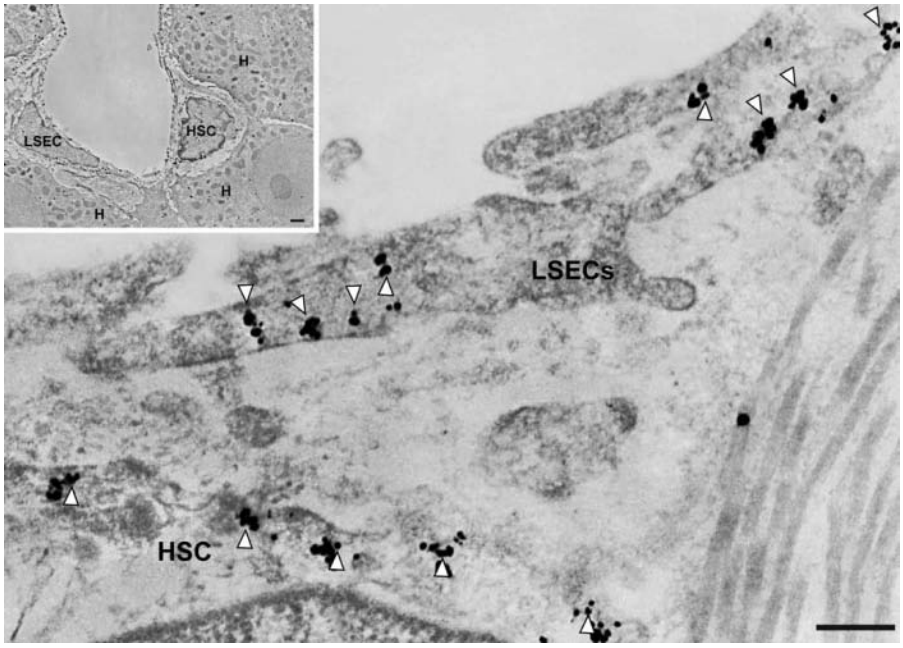

Figure 8. Transmission electron micrographs showing capillary, vascular, and liver sinusoidal endothelial cells in cirrhotic liver tissue. In cirrhotic liver, the thin endothelial lining is closed by a diaphragm. A continuous basal lamina can be seen underneath the endothelium. Immunogold particles indicating caveolin-1 are found on vesicles and caveolae in capillarized liver sinusoidal endothelial cells. LSEC, liver sinusoidal endothelial cell; HSC, hepatic stellate cell; H, hepatocyte. Magnification: ×20,000 (bar: 200 nm). Inset shows lower magnification: ×2000 (bar: 1 μm). White arrowhead denotes caveolae-like structure.

normal sinusoids (Wisse et al. 2010). Actually, caveolin-1 is expressed in non-coated vesicles but not in clathrin-coated vesicles. Consequently, the two types of vesicles definitely have different structures as well as functions. In this study, caveolin-1 was localized in caveola-like structures in cirrhotic LSECs. This phenomenon might be caused by increased portal blood flow and augmented intrahepatic vascular resistance due to capillarization of hepatic sinusoids (loss of endothelial fenestrations and collagen deposition in the space of Disse). However, the relationship between various types of vesicles have to be elucidated in future investigations.

In conclusion, in this study, the ultrastructural localization of caveolin-1 in human LSECs at the immunoelectron microscopic level was unambiguously demonstrated. Moreover, a direct relation between caveolin-1 upregulation and progression of human hepatitis C cirrhosis via sinusoidal capillarization could be drawn from this study.

Declaration of Conflicting Interests

The authors declared a potential conflict of interest (e.g. a financial relationship with the commercial organizations or products discussed in this article) as follows: Hiroaki Yokomori received research grants from MSD, Chugai pharmaceutical Co. Ltd,

Daiichi Sankyo Co. Ltd., Dainippon Sumitomo Pharma Co., Ltd., Zeria Pharmaceutical Co. Ltd., Otsuka Pharmaceutical Co. Ltd, and lecture fees from Otsuka Pharmaceutical Co. Ltd.

Funding

The authors disclosed receipt of the following financial support for the research and/or authorship of this article: Hiroaki Yokomori received research grants from MSD, Chugai Pharmaceutical Co. Ltd, Daiichi Sankyo Co. Ltd., Dainippon Sumitomo Pharma Co., Ltd., Zeria Pharmaceutical Co. Ltd., Otsuka Pharmaceutical Co. Ltd, and lecture fees from Otsuka Pharmaceutical Co. Ltd.

References

Bardadin KA, Desmet VJ. 1985. Ultrastructural observations on sinusoidal endothelial cells in chronic active hepatitis. Histopathology. 9:171–181.

Baschong W, Stierhof YD. 1998. Preparation, use, and enlargement of ultrasmall gold particles in immunoelectron microscopy. Microsc Res Tech. 42:66–79.

Biazik J.M, Jahn KA, Braet F. 2011. Caveolae and caveolin-1 in reptilian liver. Micron. 42:656–661.

Boyd NL, Park H, Yi H, Boo YC, Sorescu GP, Sykes M, Jo H. 2003. Chronic shear induces caveolae formation and alters ERK and Akt responses in endothelial cells. Am J Physiol Heart Circ Physiol. 285: H1113–H1122.

Davies PF. 1995. Flow-mediated endothelial mechanotransduction. Physiol Rev. 75:519–560.

Griffoni C, Spisni E, Santi S, Riccio M, Guarnieri T, Tomasi V. 2000. Knockdown of caveolin-1 by antisense oligonucleotides impairs angiogenesis in vitro and in vivo. Biochem Biophys Res Commun. 276:756–761.

Hendrickson H, Chatterjee S, Cao S, Morales Ruiz M, Sessa WC, Shah V. 2003. Influence of caveolin on constitutively activated recombinant eNOS: insights into eNOS dysfunction in BDL rat liver. Am J Physiol Gastrointest Liver Physiol. 285:G652–G660.

Humbel BM, Sibon OC, Stierhof Y-D, Schwarz H. 1995. Ultrasmall gold particles and silver enhancement as a detection system in immunolabeling and in situ hybridization. J Histochem Cytochem. 43:735–737.

Ito Y, Sørensen KK, Bethea NW, Svistounov D, McCuskey MK, Smedsrod BH, McCuskey RS. 2007. Age-related changes in the hepatic microcirculation in mice. Exp Gerontol. 42:789–797.

Iwamura S, Enzan H, Saibara T, Onishi S, Yamamoto Y. 1994. Appearance of sinusoidal inclusion-containing endothelial cells in liver disease. Hepatology. 20:604–610.

Lam CM, Fan ST, Lo CM, Wong J. 1999. Major hepatectomy for hepatocellular carcinoma in patients with an unsatisfactory indocyanine green clearance test. Br J Surg. 86:1012–1017.

Liu J, Wang XB, Park DS, Lisanti MP. 2002. Caveolin-1 expression enhances endothelial capillary tubule formation. J Biol Chem. 277:10661–10668.

Ogi M, Yokomori H, Oda M, Yoshimura K, Nomura M, Ohshima S, Akita M, Toda K, Ishii H. 2003. The localization and distribution of caveolin-1 of sinusoidal cells in rat liver. Med Electron Microsc. 36:33–40.

Parton RG, Simons K. 2007. The multiple faces of caveolae. Nat Rev Mol Cell Biol. 8:185–194.

Rajamannan NM, Springett MJ, Pederson LG, Carmichael SW. 2002. Localization of caveolin 1 in aortic valve endothelial cells using antigen retrieval. J Histochem Cytochem. 50:617–627.

Rothberg KG, Heuser JE, Donzell WC, Ying YS, Glenney JR, Anderson RGW. 1992. Caveolin, a protein-component of caveolae membrane coats. Cell. 68:673–682.

Sawada H, Esaki M. 1993. Use of Nanogold followed by silver enhancement and gold toning for postembedding immunolocalization in osmium-fixed, Epon-embedded tissues. J Electron Microsc. 43:361–366.

Sawada H, Esaki M. 2000. A practical technique to postfix nanogold-immunolabeled specimens with osmium and to embed them in Epon for electron microscopy. J Histochem Cytochem. 48:493–498.

Schledzewski K, Géraud C, Arnold B, Wang S, Gröne HJ, Kempf T, Wollert KC, Straub BK, Schirmacher P, Demory A, et al. 2011. Deficiency of liver sinusoidal scavenger receptors stabilin-1 and -2 in mice causes glomerulofibrotic nephropathy via impaired hepatic clearance of noxious blood factors. J Clin Invest. 121:703–714.

Schnitzer JE, Siflinger-Birnboim A, Del Vecchio PJ, Malik AB. 1994. Segmental differentiation of permeability, protein glycosylation, and morphology of cultured bovine lung vascular endothelium. Biochem Biophys Res Commun. 199:11–19.

Smedsrød B, Kjellén L, Pertoft H. 1985. Endocytosis and degradation of chondroitin sulphate by liver endothelial cells. Biochem J. 229:63–71.

Yazama F, Esaki M, Sawada H.1997. Immunocytochemistry of extracellular matrix components in the rat seminiferous tubule: electron microscopic localization with improved methodology. Anat Rec. 248:51–62.

Yokomori H, Oda M, Ogi M, Tsukada N, Ishii H. 2002. Enhanced expression of endothelial nitric oxide synthase and caveolin-1 in human cirrhosis. Liver. 22:150–158.

Yokomori H, Oda M, Yoshimura K, Kaneko F, Hibi T. 2011. Aquaporin-1 associated with hepatic arterial capillary proliferation on hepatic sinusoid in human cirrhotic liver. Liver Int. 31:1554–1564.

Yokomori H, Oda M, Yoshimura K, Nagai T, Fujimaki K, Watanabe S, Hibi T. 2009. Caveolin-1 and Rac regulate endothelial capillary-like tubular formation and fenestral contraction in sinusoidal endothelial cells. Liver Int. 29:266–276.

Warren A, Cogger VC, Arias IM, McCuskey RS, Le Couteur DG. 2010. Liver sinusoidal endothelial fenestrations in caveolin-1 knockout mice. Microcirculation. 17:32–38.

Wisse E. 1972. An ultrastructural characterization of the endothelial cell in rat liver sinusoids under normal and various experimental conditions, as a contribution to the distinction between endothelial and Kupffer cells. Ultrastruct Res. 38:528–562.

Wisse E, Braet F, Duimel H, Vreuls C, Koek G, Olde Damink SW, van den Broek MA, De Geest B, Dejong CH, Tateno C, et al. 2010. Fixation methods for electron microscopy of human and other liver. World J Gastroenterol. 16:2851–2866.